

Framework for embedding black-box simulation into mathematical programming via kriging surrogate model applied to natural gas liquefaction process optimization

Chemical Engineering Department, State University of Maringá, Maringá, Brazil

^a Lucas F. Santos^{a*}, Caliane B. B. Costa^a, José A. Caballeró^b, Mauro A. S. S. Ravagnani^c

Chemical Engineering Department, University of Alicante, Alicante, Spain

Abstract

This paper presents a framework to solve the constrained black-box simulation optimization problem that arises from the optimal energy-efficient design of single-mixed refrigerant natural gas liquefaction process using reliable process simulator. Kriging surrogate model is used to introduce simple, computationally inexpensive, and effective algebraic formulations with reliable derivatives to the black-box objective and constraints functions. The algebraic surrogate optimization problem is embed into a nonlinear programming (NLP) model in GAMS. The NLP problem is solved using efficient multi-start gradient-based optimization with CONOPT local solver to determine a candidate of decision variables for which the true functions are calculated in the rigorous simulation. The single-mixed refrigerant process is analyzed considering 1-to-3-stage expansion and phase separation to assess potential energy savings. The present approach results show that more expansion stages can provide energy savings from 10.02 to 14.71 % comparing 2-stage and 3-stage expansion system with 1-stage. This optimization framework is more effective and consistent than Particle Swarm Optimization and Genetic Algorithm given the same budget of simulation evaluations for the considered simulation optimization problems resulting in 12.02 to 34.69 % savings.

Keywords: Simulation optimization, Kriging, Process simulation, Surrogate-based optimization, Natural gas liquefaction, Mathematical programming.

1. Introduction

Modeling and simulating complex systems rigorously with pure symbolic formulations and analytical methods can become very complicated with increasing size and complexity of the model, which can be a system of nonlinear algebraic or algebraic-differential equations. Therefore, much of today's engineering applications uses rigorous computer codes (simulation) to describe complex systems employing state-of-the-art numerical methods, in a black-box fashion [1]. In other words, for a given input $\mathbf{x} \in \mathbb{R}^n$, the simulation calculates the response variables of interest $\mathbf{y} \in \mathbb{R}^p$, in which n and p are the number of independent and dependent variables in the simulation, respectively. Although very efficient to describe in details complex

*Corresponding author:

Email address: lfs.francisco.95@gmail.com, pg54347@uem.br (Lucas F. Santos)

9 systems that would otherwise have to be simplified or approximated, a drawback of using black-box models
 10 is the lack of symbolic formulation of the model equations and the analytical derivatives that are useful
 11 for optimization, for example. The use of simulation may also introduce noise to the calculations due to
 12 convergence and approximations of numerical methods [2]. In that sense, the optimization models that
 13 require simulations to calculate the objective function and/or constraints are often referred to as simulation
 14 optimization problem [3]. A simplified version of this class of problems can be described as to find an $\mathbf{x}^* \in \mathbb{R}^n$
 15 that solves globally the following constrained problem

$$\begin{aligned} \min_{\mathbf{x} \in \mathcal{D}} f(\mathbf{x}) \\ \text{s.t. } \mathbf{g}(\mathbf{x}) \leq 0, \end{aligned} \tag{1}$$

16 in which the objective function $f : \mathbb{R}^n \mapsto \mathbb{R}$ and constraints $\mathbf{g} : \mathbb{R}^n \mapsto \mathbb{R}^q$, in which q is the number of
 17 constraints, are somewhat expensive to calculate, slightly noisy, and black-box functions, *i.e.* there is no
 18 available mathematical expression for f or \mathbf{g} , but for a given $\mathbf{x} \in \mathcal{D} \subseteq \mathbb{R}^n$ the value of $f(\mathbf{x})$ and $\mathbf{g}(\mathbf{x})$
 19 are calculated in a computer code simulation with some noise. Besides being expensive to calculate and
 20 black-box, these functions that relies on the simulation can be noisy due to numerical approximations and
 21 convergence tolerance, which can jeopardize the calculation of accurate approximate derivatives and, there-
 22 fore, the use of gradient-based optimization methods directly [2]. Also, the lack of analytical formulations of
 23 the optimization problem prevents the derivation of rigorous upper and lower bounds of the functions that
 24 are used for deterministic global optimization [4].

25 Knowing that the functions in the simulation optimization problem as in Eq. (1) are expensive to calcu-
 26 late, black-box, and noisy, methods like gradient-based with stochastic approximation, direct search, random
 27 search, and response surface are suited to solve it [3]. The latter group of methods, also known as surrogate-
 28 based optimization, has shown promising results in recent years [5]. The main idea behind these methods is
 29 to construct surrogate models, also known as meta-models or response surfaces, of the simulation-dependent,
 30 black-box functions from the optimization problem. These cheaper-to-evaluate surrogate functions are used
 31 to determine a candidate solution of the black-box optimization problem via optimization of either an acqui-
 32 sition function or the surrogate functions directly [6]. The latter approach has been investigated extensively
 33 with important classic works. For instance, Kushner [7] considered the probability of improvement to find
 34 promising next iterates to optimize the unknown function. Sacks et al. [8] analyzed maximizing the inte-
 35 grated mean squared error, the maximum mean squared error, and entropy of the surrogate model to guide
 36 the search. Jones et al. [9] used an efficient global optimization approach to the expected improvement
 37 acquisition function. Schonlau et al. [10] developed a general acquisition function for the constrained prob-
 38 lem, which is a generalization of the expected improvement criterion averaged by the joint probability of
 39 constraints being feasible.

40 More recently, boosted by recent advances in machine learning models, the surrogate-based optimization
 41 approaches that solves the surrogate optimization problem directly to guide the search toward the opti-

mization of the true functions have gained popularity. Besides machine learning models, such as artificial neural networks, random forests, radial basis functions, polynomials, etc., the kriging [11] surrogate model has driven researchers’ attention as it is an interpolating model, which has few parameters to adjust, is cheap to evaluate, and has explicit algebraic formulation. Some important contributions to this surrogate-based optimization field of research includes Davis and Ierapetritou [12], which developed a kriging-based optimization with response surface model optimization for local refinement. Caballero and Grossmann [2] proposed a trust-region algorithm using kriging surrogate models of slightly noisy black-box functions embedded with implicit (non-noisy simulation functions) and algebraic equations in nonlinear programming (NLP) problems and solved each sub-problem with SNOPT solver. The approach was applied to the design of distillation columns, sequence of distillation columns, and production of phthalic anhydride from o-xylene. Cozad et al. [13] proposed the ALAMO software, which uses a global mixed-integer nonlinear programming (MINLP) approach to symbolic regression considering an ensemble of surrogates and aiming simple function formulation that can be efficiently used for optimization. Boukouvala and Floudas [4] developed an iterative framework, called ARGONAUT, composed by bounds tightening, sampling, surrogate function selection, global optimization of the surrogate-embedded NLP problem using ANTIGONE solver, and collection of new sampling points until convergence. Wang and Ierapetritou [14] proposed a kriging-based framework for the optimization of stochastically constrained problems. The main contribution of this work was to present the “feasibility-enhanced Expected Improvement” acquisition function, which explicitly improves the feasibility knowledge while searching for a new sample point. Quirante et al. [15] embedded process simulator to generalized disjunctive programming problems considering integer variables and using kriging surrogate model for noisy black-box functions and implicit equations for non-noisy ones. The logic-based Outer Approximation solver was employed with SNOPT for NLP sub-problems using TOMLAB-MATLAB interface, and the approach was applied to the synthesis of vinyl chloride monomer production process. Schweidtmann and Mistos [16] proposed the MAiNGO software, which is a deterministic global optimization solver for NLP problems with artificial neural networks surrogate models embedded. The solver uses McCormick relaxations in a reduced space employing the convex and concave envelopes of the nonlinear activation function. The framework was tested on four optimization examples: an illustrative function, a fermentation process, a compressor plant and the cumene production process. Thebelt et al. [17] developed a framework, called ENTMOOT, for embedding trained gradient boosted trees surrogate models into larger NLP problems and tested it on constrained global optimization test problems and on a fermentation process. Kim and Boukouvala [18] proposed a framework to simulation-based MINLP problems that uses adaptive sampling and surrogate modeling with one-hot encoding (without integer variables relaxation) that resulted in accurate and robust mixed-variable kriging and neural network models, which were effective surrogates for optimization. The approach was tested on MINLP benchmark problems and a chemical process synthesis case study.

77 One application of simulation optimization problem is in the design of natural gas liquefaction processes.
78 These cryogenic refrigeration processes consist of cooling down the natural gas to about -160 °C at slightly
79 above ambient pressure to liquefy, store, transport, and commercialize it safely [19]. These processes consume
80 significant amounts of energy and their optimal design are very important to reduce the cost of liquefied
81 natural gas (LNG) as its liquefaction is responsible for 40–60 % of the costs of the LNG value chain, depending
82 on the site conditions and available liquefaction technology [20]. Also, they are of extreme importance
83 currently as the natural gas demand is expected to increase 29.4 % from 2019 to 2040, accordingly to the
84 International Energy Agency [21]. This expected increase in natural gas demand is mainly due to the
85 increasingly global energy consumption, which is expected to go from 603 to 715 trillion MJ per year from
86 2019 to 2040 [21], and for it being a cleaner and economically competitive energy source compared to other
87 fossil fuels, such as oil and coal.

88 The natural gas liquefaction process that uses a mixture operating in a single refrigeration cycle and
89 explores its temperature range of evaporation as heat sink to cool and liquefy both the natural gas stream
90 and itself in a multi-stream heat exchanger (MSHE) is called single-mixed refrigerant (SMR) process. From
91 the simulation point of view, the main modeling challenges in this process come from the vapor-liquid
92 equilibrium calculations at below ambient temperature and the Pinch-like calculation in the multi-stream
93 heat exchangers considering phase change and rigorous thermodynamic calculations at cryogenic conditions.
94 Therefore, it is useful to employ chemical process simulators, where all of these difficult calculations are
95 performed with state-of-the-art methods, equations, and empirical coefficients. The optimization part of
96 the problem consists of choosing the process degrees of freedom, such as refrigerant composition and the
97 thermodynamic cycle conditions to improve a process metric of interest. For that, optimization techniques
98 have been used extensively in the past decade, as reported in the annotated bibliography from Austbø et al.
99 [22].

100 Some of the important contributions on optimal design of SMR natural gas liquefaction process that
101 used optimization techniques to reliable black-box process simulator are now reviewed. Lee [23] developed a
102 sequential methodology for the systematic synthesis of mixed-refrigerant systems by a combined mathemat-
103 ical programming and thermodynamic approach and applied to the SMR liquefaction process with 1-stage
104 compression and multi-stage expansion. Nogal et al. [24] investigated, using a Genetic Algorithm (GA),
105 the optimal design of mixed refrigerant cycles that included multistage refrigerant compression, 1-to-4-stage
106 expansion, multiple refrigeration cycles, full enforcement of the minimum temperature difference in heat
107 exchangers, simultaneous optimization of variables, and consideration of capital costs. Aspelund et al. [25]
108 tackled the optimal design of SMR process for natural gas liquefaction with 1-stage compression and 1-stage
109 expansion using a hybrid optimization approach of Taboo Search and Nelder-Mead algorithm. Wahl et al.
110 [26] investigated the optimization of a simple 1-stage compression and 1-stage expansion SMR natural gas liq-
111 uefaction process using a time-efficient Sequential Quadratic Programming routine connected to the process

112 simulator. Hwang et al. [27] proposed a generic liquefaction superstructure model to express various types
113 of liquefaction cycles, from which 27 feasible configurations were optimized to reduce compression power
114 consumption. Thermodynamic calculations were in sequential modular fashion, using the Peng-Robinson
115 equation of state, and a hybrid optimization framework consisting of GA and SQP was used. Khan and Lee
116 [28] investigated the effectiveness of Particle Swarm Optimization (PSO) in simulation optimization problems
117 in the optimal design of SMR natural gas liquefaction process with 4-stage compression and 1-stage expan-
118 sion. He et al. [29] proposed and optimized a novel SMR cycle integrated with **natural gas liquids** recovery
119 process for small-scale LNG plant using a GA. Khan et al. [30] investigated the performance of a sequential
120 coordinate randomization search method for optimizing SMR natural gas liquefaction process. Moein et al.
121 [31] minimized total required work of the commercial APCI-SMR natural gas liquefaction process, which
122 includes a 3-stage compression with phase separation and a 3-stage expansion systems, using a GA. Park
123 et al. [32] optimized the Korea SMR process, which considers a 3-stage compression with phase separation
124 and 2-stage expansion systems and 2-phase expander for LNG stream, using a modified coordinate descent
125 methodology. Austbø and Gundersen [22] minimized the power consumption of a simple 1-stage compression
126 and 1-stage expansion SMR process for natural gas liquefaction using four different constraint formulations
127 to handle the trade-off between investment and operating costs using SQP with multiple starting points.

128 More recently, Pham et al. [33] developed a knowledge-inspired hybrid optimization of a modified SMR
129 natural gas liquefaction process with 2-stage compression with phase separation and 2-stage expansion with-
130 out phase mixing targeted for offshore applications. Na et al. [34] analyzed the performance of a modified
131 DIRECT algorithm to optimize **an** SMR natural gas liquefaction process with 3-stage compression and 2-
132 stage expansion. Pham et al. [35] investigated the energy enhancement of SMR natural gas liquefaction
133 process with 4-stage compression with phase separation and 1-stage expansion using knowledge-based opti-
134 mization. Qyyum et al. [36] investigated the effect of replacing the throttling valve of Joule-Thomson effect
135 with hydraulic turbine in the energy efficiency enhancement of **an** SMR natural gas liquefaction process with
136 4-stage compression and 1-stage expansion. Qyyum et al. [37] analyzed the performance of a hybrid modified
137 coordinate descent algorithm to cope with the optimization of **an** SMR natural gas liquefaction process with
138 4-stage compression with phase separation and 1-stage expansion. Ali et al. [38] investigated the performance
139 of a meta-heuristic vortex search algorithm for the optimization of **an** SMR natural gas liquefaction process
140 with 4-stage compression with phase separation and 1-stage expansion. Ali et al. [39] examined surrogate-
141 assisted modeling and optimization of the SMR natural gas liquefaction process with 4-stage compression and
142 1-stage expansion. The process optimization was carried out using a surrogate-assisted modeling approach
143 that was optimized using GA and PSO. Lee et al. [40] performed, **using a GA, the** design and optimization
144 of 3-stage compression with phase separation and 1-stage expansion SMR natural gas liquefaction process
145 **with several steady-state operation regimes**, depending on the load variation using a GA. He et al. [41]
146 proposed a comprehensive optimization and comparison between 2-stage compression with phase separation

147 and 2-stage expansion SMR and parallel nitrogen expansion natural gas liquefaction processes from the per-
148 spectives of specific energy consumption, exergy efficiency, techno-economy, and operational flexibility using
149 a GA. Qyyum et al. [42] proposed an energy-and-cost-efficient 2-stage expansion SMR process for natural
150 gas liquefaction and compared it to the dual-mixed-refrigerant process. Nikkho et al. [43] optimized two
151 mini-scale modified 3-stage compression with phase separation, 2-stage expansion SMR natural gas lique-
152 faction processes using a GA. Santos et al. [44] investigated the optimization of a 4-stage compression with
153 phase separation, 1-stage expansion SMR natural gas liquefaction process employing an augmented number
154 of decision variables with Nelder-Mead derivative-free optimization method, considering valve and hydraulic
155 turbine expansion. Later the methodology was improved in Santos et al. [45], in which a kriging-assisted
156 global search scheme that included the optimization of the probability of feasible improvement acquisition
157 function to find promising candidates to run the local search with Nelder-Mead algorithm.

158 Most of the present literature on optimal design of the SMR natural gas liquefaction process have re-
159 lied on global optimization meta-heuristics, mainly GA, to investigate more sophisticated aspects of the
160 processes, such as energy-efficient, robust, and flexible design, process flow diagram modifications, and eco-
161 nomic analysis. Although meta-heuristics are powerful tools for complex optimization problems [46], these
162 methods usually require lots of functions evaluations and lack deterministic convergence proof. Given the
163 present review on methods for black-box optimization problems and single-mixed refrigerant natural gas
164 liquefaction process design and considering the particularities of the simulation optimization problem from
165 this design task toward minimum energy consumption using reliable chemical process simulators, surrogate
166 modeling can be used to introduce symbolic formulation to the optimization problem functions that then
167 can be embedded in mathematical programming setup and solved using classical and efficient gradient-based
168 optimization or deterministic global optimization. Differently from what was done in [39] and [45], which
169 optimized the surrogate optimization problem or acquisition function based on the surrogate models using
170 global optimization meta-heuristics, the present approach explore the mathematical information introduced
171 by the surrogate models. It means that, generic regression models are fitted to data generated from the rig-
172 orous simulation and used to replace the black-box functions f and \mathbf{g} by surrogates \hat{f} and $\hat{\mathbf{g}}$ that introduce
173 analytical formulation to those functions with reliable derivatives that can be used for efficient gradient-based
174 optimization of the resulted nonlinear programming problem.

175 The objective of the present paper is to propose an effective utilization of kriging surrogate models
176 to replace the process-simulator-dependent, black-box objective and constraints functions and introduce
177 explicit algebraic formulation to the optimization problem. The proposed framework consists of a three-
178 piece program: the main program in MATLAB that stores the sampled data at the rigorous simulation-
179 dependent functions, fits and updates the kriging models, calls the process simulator for rigorous function
180 evaluations of candidates, and calls GAMS for solving the surrogate optimization nonlinear programming
181 problem; the simulator program in Aspen HYSYS that contains the processes models and calculates the

182 rigorous functions of the optimization problem; and the algebraic modeling system in GAMS that contains
183 the surrogate optimization problem implemented explicitly, receives the current NLP problem parameters
184 from the main program, and returns the solution to it. One novelty of the present approach to make the
185 liquefaction process simulation optimization effective using surrogate models is to divide the multi-stream
186 heat exchangers, which are modeled like Pinch calculations with phase change and non-ideal solutions, so
187 that the temperature driving force between hot and cold composite curves are calculated for each segment
188 of the heat exchanger instead of the whole. This leads to better behaved functions that are well adjusted by
189 the surrogate models for the sake of optimization.

190 To test the optimization methodology, the single-mixed refrigerant natural gas liquefaction process de-
191 sign considering 1, 2, and 3 expansion stages is investigated. The decision variables in these simulation
192 optimization problems are the refrigerant component flow rate, the condensation and evaporation pressure,
193 and the expansion temperature of the multi-component refrigerant in the refrigeration cycle. The considered
194 constraint is that a minimum temperature driving force of 3 °C must be assured throughout every multi-
195 stream heat exchanger. Also, phase separation is considered in between compression stages to explore the
196 energy savings from condensation along the refrigeration cycle. The optimization results from the present
197 methodology are compared with two global meta-heuristic optimization approach, which are Particle Swarm
198 Optimization and Genetic Algorithm. The energy efficiency of multi-stage expansion is investigated jointly
199 with a thermodynamic analysis of entropy generation. The computational aspects of the present approach is
200 analyzed with respect to prediction time of the kriging models, and convergence of the proposed algorithm.

201 This paper is organized so that in Section 2 the kriging model and the surrogate optimization problem
202 are defined and derived. Section 3 describes in detail the single-mixed refrigerant natural gas liquefaction
203 process with 1-to-3-stage expansion system as well as its simulation considerations, constraints, degrees of
204 freedom, and optimization. Section 4 presents the optimization framework that includes sampling, kriging
205 model fitting, and efficient derivative-based optimization of the surrogate problem. Section 5 provides the
206 results of the present optimization approach to the natural gas liquefaction design problem, jointly with an
207 energy and thermodynamic efficiency analysis of multi-stage expansion, a performance comparison with two
208 well-established meta-heuristic for global optimization, Particle Swarm Optimization and Genetic Algorithm,
209 and the computational aspects of the algorithm.

210 2. Kriging-based constrained optimization

211 To solve the black-box constrained simulation optimization problems as in Eq. (1), a framework that uses
212 kriging models as surrogates of the objective function f and constraints \mathbf{g} to introduce a simple and efficient
213 algebraic formulation of the black-box functions for efficient gradient-based optimization is presented in this
214 section. The first step of this method is to derive the kriging model of f and \mathbf{g} . For simplicity, in Sections
215 2.1, the kriging model is derived only for f , but the same process can be extended easily for \mathbf{g}_i , $i = 1, \dots, q$. In

216 Section 2.2 the surrogate optimization problem in algebraic form is derived, which is implemented in GAMS
 217 to be solved with state-of-the-art optimization solvers.

218 2.1. Kriging Model

219 For mathematical background on the surrogate model used in this surrogate-based optimization frame-
 220 work, the kriging model is derived as the best linear unbiased predictor, Gaussian process regression model
 221 following the derivation of Sacks et al. [8], Lophaven et al. [47], Stein [48], and Santos et al. [45].

222 First, consider the following regression

$$\hat{f}(\mathbf{x}) = \boldsymbol{\beta}^T \mathcal{F}(\mathbf{x}) + z(\mathbf{x}) \quad (2)$$

223 in which $\mathcal{F} : \mathbb{R}^n \mapsto \mathbb{R}^p$ is a combination of p linear or nonlinear functional forms that approximates f , $\boldsymbol{\beta} \in \mathbb{R}^p$
 224 are the p regression coefficients, and z is the error between the true function and the regression model given
 225 by a stochastic function with zero mean and covariance between two points $z(\mathbf{x}^{(i)})$ and $z(\mathbf{x}^{(j)})$ given by

$$\text{cov} \left(z(\mathbf{x}^{(i)}), z(\mathbf{x}^{(j)}) \right) = \sigma^2 \mathcal{R}(\boldsymbol{\theta}, \mathbf{x}^{(i)}, \mathbf{x}^{(j)}),$$

226 where σ^2 is the process variance and $\mathcal{R}(\boldsymbol{\theta}, \mathbf{x}^{(i)}, \mathbf{x}^{(j)})$ is the correlation model with parameters $\boldsymbol{\theta} \in \mathbb{R}^n$.
 227 Now, assuming some continuity about the function f , one would expect that the correlation between points
 228 that are closer to each other is greater than those that are far apart. That notion is translated into the
 229 correlation model. There are many correlation models, also known as kernels, that obey this intuition (see
 230 [8] for more details), and in this work the Gaussian correlation is used

$$\mathcal{R}(\boldsymbol{\theta}, \mathbf{x}^{(i)}, \mathbf{x}^{(j)}) = \exp \left[- \sum_{h=1}^n \boldsymbol{\theta}_h \left(\mathbf{x}_h^{(i)} - \mathbf{x}_h^{(j)} \right)^2 \right], \quad (3)$$

231 where $\boldsymbol{\theta}_h > 0$ is the h^{th} component of the parameters that scales how the correlation between points changes
 232 with respect to the h^{th} component of their distance squared.

233 In the present paper, the regression model chosen is $\mathcal{F}(\mathbf{x}) = 1$, so that $p = 1$ and the kriging predictor is
 234 called ordinary kriging. This regression model simplicity usually is enough for good prediction [2] because
 235 the behavior of the data is incorporated in the error model $z(\mathbf{x})$. Now, suppose there are m sampled
 236 points $\mathbf{X} = [\mathbf{x}^{(1)} \dots \mathbf{x}^{(m)}]^T$, where $\mathbf{x}^{(i)} \in \mathcal{D} \subseteq \mathbb{R}^n, \forall i = 1, \dots, m$ is the i^{th} sampled point. And, for
 237 all these points, the value of $y^{(i)} \in \mathbb{R} \mid y^{(i)} = f(\mathbf{x}^{(i)}), \forall i = 1, \dots, m$ so that $\mathbf{Y} = [y^{(1)} \dots y^{(m)}]^T$ and
 238 $\mathbf{g}^{(i)} \in \mathbb{R}^q \mid \mathbf{g}^{(i)} = \mathbf{g}(\mathbf{x}^{(i)}), \forall i = 1, \dots, m$ so that $\mathbf{G} = [\mathbf{g}^{(1)} \dots \mathbf{g}^{(m)}]^T$ are available. Then, it is possible to define
 239 $\mathbf{R}(\boldsymbol{\theta}) \in \mathbb{R}^{m \times m}$ as the matrix of stochastic-process correlations between z at sampled points, which is $\mathbf{R}_{i,j}(\boldsymbol{\theta}) =$
 240 $\mathcal{R}(\boldsymbol{\theta}, \mathbf{x}^{(i)}, \mathbf{x}^{(j)}), i, j = 1, \dots, m$, and $\mathbf{r}(\mathbf{x}, \boldsymbol{\theta}) \in \mathbb{R}^m$ such that $\mathbf{r}(\mathbf{x}, \boldsymbol{\theta}) = [\mathcal{R}(\boldsymbol{\theta}, \mathbf{x}^{(1)}, \mathbf{x}) \dots \mathcal{R}(\boldsymbol{\theta}, \mathbf{x}^{(m)}, \mathbf{x})]^T$.
 241 Finally, deriving the kriging model as the best linear unbiased predictor (see Stein [48], Lophaven et al. [47]
 242 or Santos et al. [45] for a complete derivation) in Eq. (2) becomes

$$\hat{f}(\mathbf{x}) = \hat{\beta} + \mathbf{r}(\mathbf{x})^T \mathbf{R}^{-1} (\mathbf{Y} - \mathbf{1} \hat{\beta}), \quad (4)$$

243 where, $\mathbf{1}$ is a column vector of m entries of ones,

$$\hat{\beta} = \frac{\mathbf{1}^T \mathbf{R}^{-1} \mathbf{Y}}{\mathbf{1}^T \mathbf{R}^{-1} \mathbf{1}}, \quad (5)$$

244 is the generalized least square solution of the regression coefficient,

$$\hat{\sigma}^2 = \frac{1}{m} (\mathbf{Y} - \mathbf{1} \hat{\beta})^T \mathbf{R}^{-1} (\mathbf{Y} - \mathbf{1} \hat{\beta}), \quad (6)$$

245 is the process variance, and

$$\hat{s}^2(\mathbf{x}) = \hat{\sigma}^2 \left(1 - \mathbf{r}(\mathbf{x})^T \mathbf{R}^{-1} \mathbf{r}(\mathbf{x}) + \frac{(1 - \mathbf{1}^T \mathbf{R}^{-1} \mathbf{r}(\mathbf{x}))^2}{\mathbf{1}^T \mathbf{R}^{-1} \mathbf{1}} \right), \quad (7)$$

246 is the expected mean squared error of the predictor.

247 With Eqs. (4), (5), (6), and (7) it is possible to predict the value of the function f at untried points \mathbf{x}
 248 and estimate the prediction error. It remains unknown, however, the parameters $\boldsymbol{\theta}$ of the correlation matrix
 249 in Eq. (3). Notice that an approach of minimization of prediction error to determine the model parameters
 250 is not possible because kriging as in Eq. (4) interpolates the data for any $\boldsymbol{\theta} > 0$, see Santos et al. [45]
 251 for proof to this remark. Then, those parameters are determined by maximum likelihood of the model, *i.e.*
 252 maximizing the probability of the data given the model, $p(\hat{f}(\mathbf{x})|\mathbf{x}, \boldsymbol{\theta}, \mathbf{p})$. The likelihood is given by

$$\mathcal{L}(\boldsymbol{\theta}, \mathbf{p}|\mathbf{X}, \mathbf{Y}) = \frac{1}{(2\pi)^{m/2} (\hat{\sigma}^2)^{m/2} |\mathbf{R}|^{1/2}} \exp \left[\frac{-(\mathbf{Y} - \mathbf{1} \hat{\beta})^T \mathbf{R}^{-1} (\mathbf{Y} - \mathbf{1} \hat{\beta})}{2\hat{\sigma}^2} \right]. \quad (8)$$

253 Taking the natural log of Eq. (8), substituting $\hat{\beta}$, inverting the sign, removing the constant terms and after
 254 some algebra, the maximum likelihood problem becomes

$$\min_{\boldsymbol{\theta}} \psi(\boldsymbol{\theta}) = |\mathbf{R}|^{1/m} \hat{\sigma}^2, \quad (9)$$

255 in which $|\mathbf{R}|$ is the determinant of \mathbf{R} .

256 2.2. Surrogate Optimization Problem

257 The surrogate model defined by Eqs. (4) and (5) with $\boldsymbol{\theta}$ parameters given by the solution of the problem
 258 in Eq. (9) can be written easily in symbolic formulation to be used explicitly in algebraic modeling language
 259 software, such as GAMS, where state-of-the-art global optimization solvers can be used. The kriging model
 260 in algebraic formulation becomes

$$\hat{f}(\mathbf{x}) = \hat{\beta} + \sum_{i=1}^m \alpha_i e^{-\sum_{j=1}^n \theta_j (\mathbf{x}_j - \mathbf{X}_{i,j})^2}, \quad (10)$$

261 where $\hat{\beta}$ is given by Eq. (5), and $\boldsymbol{\alpha} = \mathbf{R}^{-1} (\mathbf{Y} - \mathbf{1} \hat{\beta})$.

262 Nevertheless, the problem of interest is the constrained optimization in Eq. (1), so that one wants to find
 263 a candidate that not only is promising for minimizing f , but also meets the inequality constraints \mathbf{g} . For

264 this reason, the kriging constraints that are $\hat{\mathbf{g}}(\mathbf{x}) \leq 0$ has to be satisfied. Thus, the constrained surrogate
 265 optimization problem in algebraic form becomes

$$\begin{aligned} \min_{\mathbf{x} \in \mathcal{D}} \quad & \hat{\beta} + \sum_{i=1}^m \alpha_i e^{-\sum_{j=1}^n \theta_j (\mathbf{x}_j - \mathbf{X}_{i,j})^2} \\ \text{s.t.} \quad & \hat{\beta}_c^{(c)} + \sum_{i=1}^m \alpha_{\mathbf{c}_i}^{(c)} e^{-\sum_{j=1}^n \theta_{\mathbf{c}_j}^{(c)} (\mathbf{x}_j - \mathbf{X}_{i,j})^2} \leq 0, \quad c = 1, \dots, q. \end{aligned} \quad (11)$$

266 It is worth mentioning that for a given set of data \mathbf{X} , \mathbf{Y} , and \mathbf{G} and trained kriging models for f and \mathbf{g} , *i.e.*
 267 θ and $\theta_{\mathbf{c}}$, the parameters $\hat{\beta}$, $\hat{\beta}_c$, α , and $\alpha_{\mathbf{c}}$ are constant. Therefore, the proposed kriging-based constrained
 268 optimization methodology transforms the black-box constrained simulation optimization problem given in
 269 Eq. (1) into two simpler optimization problems that are to adjust the models parameters to the data as in
 270 Eq. (9) and optimize the constrained surrogate optimization problem to find a promising candidate as in
 271 Eq. (11).

272 3. Natural gas liquefaction process

273 The case study and motivating problem for the proposed kriging-based optimization framework is the
 274 optimal design of single-mixed refrigerant natural gas liquefaction processes. These processes consist of
 275 using a multi-component refrigerant operating in a refrigeration cycle to produce heat sink to cool down and
 276 liquefy the natural gas stream. The considered process flow diagram of 1-to-3-stage expansion single-mixed
 277 refrigerant natural gas liquefaction is illustrated in Figure 1. The refrigeration cycle includes a 4-stage
 278 compression system with intermediate cooling and phase separation for possible condensate. The liquid
 279 phase is compressed in the pumps P-1, P-2, P-3, and P-4 and the vapor phase in the compressors K-1, K-2,
 280 K-3 and K-4. No phase mixing is considered, which means that the refrigerant heavy condensate is mixed
 281 together and goes through the hot pass in the multi-stream heat exchanger separately from the light vapor
 282 phase. Then, the streams are mixed back together in the cold pass inside the cryogenic heat exchanger
 283 as they vaporize. The third expansion stage is possible thanks to a phase separation of stream 11v, for
 284 which the condensed phase is sub-cooled and expanded in valve V-3, whereas the lighter vapor phase is first
 285 liquefied then sub-cooled to be expanded in valve V-4.

286 3.1. Process Simulation

287 The described single-mixed refrigerant natural gas liquefaction processes is rather difficult to model and
 288 simulate mainly because it involves Pinch-like calculations in each multi-stream heat exchangers considering
 289 phase change, cryogenic conditions, and non-ideal mixtures. In other words, these heat exchangers are
 290 discretized in energy segments, where vapor-liquid equilibrium calculations are performed to determine the
 291 temperature of every stream and, therefore, the temperature profiles in these operation units. And, for the
 292 sake of process feasibility considering the Second Law of Thermodynamics, the hot streams temperatures

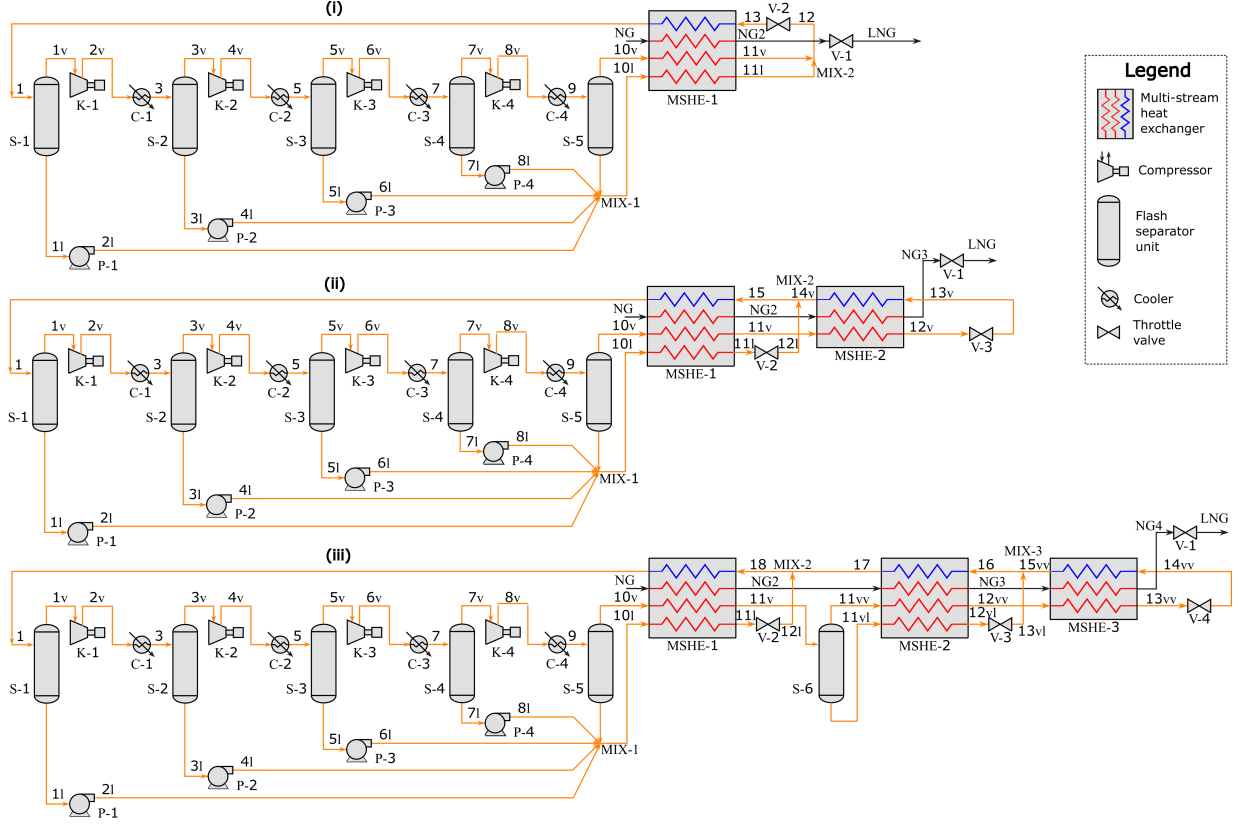


Figure 1: Process flow diagram of single-mixed refrigerant natural gas liquefaction process with 4-stage, phase-separated compression system and 1-to-3-stage expansion system, respectively in (i), (ii), and (iii).

293 have to be effectively higher than the cold ones throughout the heat exchangers. For rigorous calculations,
 294 these processes are modeled and simulated in Aspen HYSYS® V9 using Peng-Robinson equation of state,
 295 which is appropriate for hydrocarbons mixtures, such as the natural gas and the refrigerant mixtures.

296 The natural gas stream NG is considered to be at 8,000 kPa and 32 °C, and its composition is presented
 297 in Table 1 as well as other simulation parameters and considerations. A basis of calculation of 1 kg h⁻¹ for
 298 the natural gas mass flow rate is used. The refrigerant is a mixture of nitrogen, methane, ethane, propane,
 299 and i-pentane, and their component mass flow rates are optimization decision variables. The discharge and
 300 suction pressures of the multi-stage compression P_{dis} and P_{suc} are decision variables of the optimization
 301 problem, and the pressure ratio of each compression stage is given by $(P_{dis}/P_{suc})^{1/4}$, which is the ratio
 302 between the discharge and suction pressures divided by 4 stages in series. Notice that the pressure of vapor
 303 streams –subscript v – matches the liquid ones –subscript l – from 1 to 8. Finally, the temperatures of
 304 every hot stream leaving a multi-stream heat exchanger are considered to be the same to match practical
 305 constructions. The expansion temperatures are also degrees of freedom in the simulation and decision
 306 variables in the optimization problem, except **the temperature of the last expansion, which** is fixed to -149.2
 307 °C to guarantee the LNG pressure, molar vapor fraction, and temperature requirements exposed in Table 1.

Table 1: Summary of simulation parameters and considerations, adapted from Pham et al. [35]

Natural gas feed condition	
Property	Condition
Temperature	32 °C
Pressure	8,000 kPa
Flow rate	1.0 kg h ⁻¹
Composition	Molar fraction
Nitrogen	0.0022
Methane	0.9133
Ethane	0.0536
Propane	0.0214
i-Butane	0.0046
n-Butane	0.0047
i-Pentane	0.0001
n-Pentane	0.0001
Design parameters and considerations	
Intermediate cooling temperature	40 °C
Intermediate cooling pressure drop	0.0 kPa
LNG molar vapor fraction	8.0 %
LNG temperature	-158.6 °C
LNG pressure	120.0 kPa
Compressor adiabatic efficiency	0.75
Pump adiabatic efficiency	0.75
Thermodynamic property package	Peng-Robinson
MSHE pressure drop (hot stream)	100.0 kPa
MSHE pressure drop (cold stream)	10.0 kPa
Minimum temperature approach	3 °C

308

309 One practical constraint in the natural gas liquefaction process is that the minimum temperature approach
310 between hot and cold composite curves throughout the multi-stream heat exchangers must be greater than
311 or equal to 3 °C to avoid Second Law of Thermodynamic violation and impractically big heat exchange
312 area [20]. Another constraint is that all molar vapor fraction in compression inlet streams must be 1, which
313 means that only vapor is allowed in compressors to avoid physical damage. However, this constraint is always
314 assured once flash separators are considered before each compression stage. Even though this adds cost to
315 the process, these separators are considered unpenalized to investigate possible energy savings due to phase
316 separation.

317 *3.2. Process Optimization*

318 Given the process description, considerations, constraints, and degrees of freedom, it is possible to define
 319 an optimization problem from which the solution are decisions for the optimal natural gas liquefaction pro-
 320 cesses. As elaborated in Section 3.1, the decision variables of this optimization are \mathbf{m}_i , $i \in REFR = \{\text{nitrogen}$
 321 (N) , methane (C_1) , ethane (C_2) , propane (C_3) , i-pentane $(iC_5)\}$ the mass flow rate of component i in the
 322 set of refrigerants $REFR$, and P_{suc} , P_{dis} , and $T_{exp\ell=1,\dots,Ne-1}$ the suction and discharge pressures and the
 323 mixed-refrigerant temperatures of expansion. **The index ℓ refers to the expansion stage**, and Ne is the total
 324 **number** of expansion stages. Then, the decision variables for all expansion scenarios are $\mathbf{x} = [\mathbf{m}_{i \in REFR},$
 325 $P_{suc}, P_{dis}, T_{exp\ell=1,\dots,Ne-1}]$, so that $\mathbf{x} \in \mathbb{R}^n$ is the input vector of decision variables to the simulation and
 326 $n = 7 + Ne - 1$ is the dimension of the problem.

327 Knowing that the work consumption is the most relevant spending in the natural gas liquefaction process,
 328 then the design problem is to find $\mathbf{x}^* \in \mathbb{R}^n$ that minimizes the following optimization problem

$$\begin{aligned} \min_{\mathbf{x} \in \mathcal{D}} f(\mathbf{x}) &= \frac{\sum_{p \in PM} W_p(\mathbf{x})}{\dot{m}_{NG}} \\ \text{s.t. } \mathbf{g}_\ell(\mathbf{x}) &= 1 - \frac{\min_{k=1,\dots,Nk} \{Th_{\ell,k}(\mathbf{x}) - Tc_{\ell,k}(\mathbf{x})\}}{3} \leq 0, \quad \ell = 1, \dots, Ne \\ \mathcal{D} &= [\mathbf{x}^{lb}, \mathbf{x}^{ub}], \end{aligned} \quad (12)$$

329 in which, for a given \mathbf{x} , $W_p(\mathbf{x})$ is the work consumption of the pressure manipulator unit p in the set of
 330 compressors and pumps PM , $Th_{\ell,k}(\mathbf{x})$ and $Tc_{\ell,k}(\mathbf{x})$ are the temperature of hot and cold composite curves
 331 in the ℓ^{th} MSHE at energy segment k , Nk is the number of energy segments in the MSHE composite curves
 332 calculations, \mathcal{D} is a box constraint for the decision variables bounded by \mathbf{x}^{lb} and \mathbf{x}^{ub} , and \dot{m}_{NG} is the mass
 333 flow rate of the natural gas stream. Notice that the value of $W_p(\mathbf{x})$ as well as $Th_{\ell,k}(\mathbf{x})$ and $Tc_{\ell,k}(\mathbf{x})$ are
 334 obtained in the black-box chemical process simulator, **and so is $f(\mathbf{x})$ and $\mathbf{g}(\mathbf{x})$** . Then, $f(\mathbf{x})$ and $\mathbf{g}(\mathbf{x})$ are
 335 known only at sampled points and make the optimization problem equivalent to Eq. (1). Table 2 presents the
 336 values chosen for lower and upper bounds of \mathbf{x} for scenarios (i), (ii), and (iii) given by $[0.33\mathbf{x}_{base}, 1.66\mathbf{x}_{base}]$,
 337 where \mathbf{x}_{base} is a heuristically determined base case. In other words, the bounds are determined to be between
 338 $2/3$ below and above the base case. Note also that most of these bounds are selected to diminish the search
 339 region toward promising regions, rather than for physical or operational constraint, and it implicates in
 340 easier optimization problem and more stable simulations convergence. In addition, the lower bound of m_N
 341 is rounded to 0 to consider the case of a heavier multi-component refrigerant, *i.e.* without nitrogen, and the
 342 expansion temperatures are adjusted to guarantee decreasing temperature from up to downstream expansion
 343 stage.

344 **The kriging model requires some continuity about the black-box function. That may not be the case for \mathbf{g}**
 345 **as reported in Santos et al. [45] because** this function is the minimum temperature driving force between the
 346 hot and cold composite curves throughout the whole multi-stream heat exchanger, where multi-component
 347 streams undergo phase change. For that, we propose to discretize each \mathbf{g}_ℓ function in K sections, which

Table 2: Lower and upper bounds on the decision variables for the three scenarios

\mathbf{x}	\mathbf{x}_{base}	1-stage expansion		2-stage expansion		3-stage expansion	
		\mathbf{x}^{lb}	\mathbf{x}^{ub}	\mathbf{x}^{lb}	\mathbf{x}^{ub}	\mathbf{x}^{lb}	\mathbf{x}^{ub}
m_N [kg·h ⁻¹]	0.250	0.000	0.415	0.000	0.415	0.000	0.415
m_{C1} [kg·h ⁻¹]	0.600	0.198	0.996	0.198	0.996	0.198	0.996
m_{C2} [kg·h ⁻¹]	1.000	0.330	1.660	0.330	1.660	0.330	1.660
m_{C3} [kg·h ⁻¹]	1.200	0.396	1.992	0.396	1.992	0.396	1.992
m_{iC5} [kg·h ⁻¹]	1.800	0.594	2.988	0.594	2.988	0.594	2.988
P_{suc} [kPa]	250.0	82.50	415.0	82.50	415.0	82.50	415.0
P_{dis} [kPa]	4000	1320	6640	1320	6640	1320	6640
T_{exp1} [°C]	-50	-	-	-83.00	-16.50	-80.00	-16.50
T_{exp2} [°C]	-110	-	-	-	-	-130.0	-80.10

348 makes it more likely to be well behaved functions. Then, the optimization problem becomes

$$\begin{aligned}
 \min_{\mathbf{x} \in \mathcal{D}} f(\mathbf{x}) &= \frac{\sum_{p \in PM} W_p(\mathbf{x})}{\dot{m}_{NG}} \\
 s.t. \quad \mathbf{g}_\kappa(\mathbf{x}) &= 1 - \frac{\min_{k \in \Omega_\kappa} \{Th_{\ell,k}(\mathbf{x}) - Tc_{\ell,k}(\mathbf{x})\}}{3} \leq 0, \quad \kappa = 1, \dots, K \times Ne \\
 \mathcal{D} &= [\mathbf{x}^{lb}, \mathbf{x}^{ub}],
 \end{aligned} \tag{13}$$

349 in which κ is the set of $K \times Ne$ divisions in \mathbf{g} , and Ω_κ is the set of the Nk points from composite curves
350 calculations that belongs to section κ . Also, the number of constraints increases from Ne to $K \times Ne$ in the
351 proposed optimization formulation.

352 4. Optimization Framework

353 A framework is proposed in this paper to solve black-box constrained optimization problems as in Eq.
354 (1), which is tested in the energy-efficient optimal design of single-mixed refrigerant natural gas liquefaction
355 processes with 1-to-3 expansion stages. This approach uses kriging surrogate models as presented in Section
356 2.1 to substitute the black-box objective function and constraints and introduce algebraic formulation to the
357 black-box problem as presented in Section 2.2. The surrogate optimization model is, then, implemented in
358 GAMS, where it is solved with state-of-the-art, derivative-based, global solvers. Figure 2 illustrates how the
359 optimization framework operates.

360 Before anything in this optimization framework, MATLAB and Aspen HYSYS are connected via object
361 linking and embedding technology using the MATLAB built-in function “actxserver” to create in its envi-
362 ronment a component object model (COM) server of the HYSYS application with the process simulation

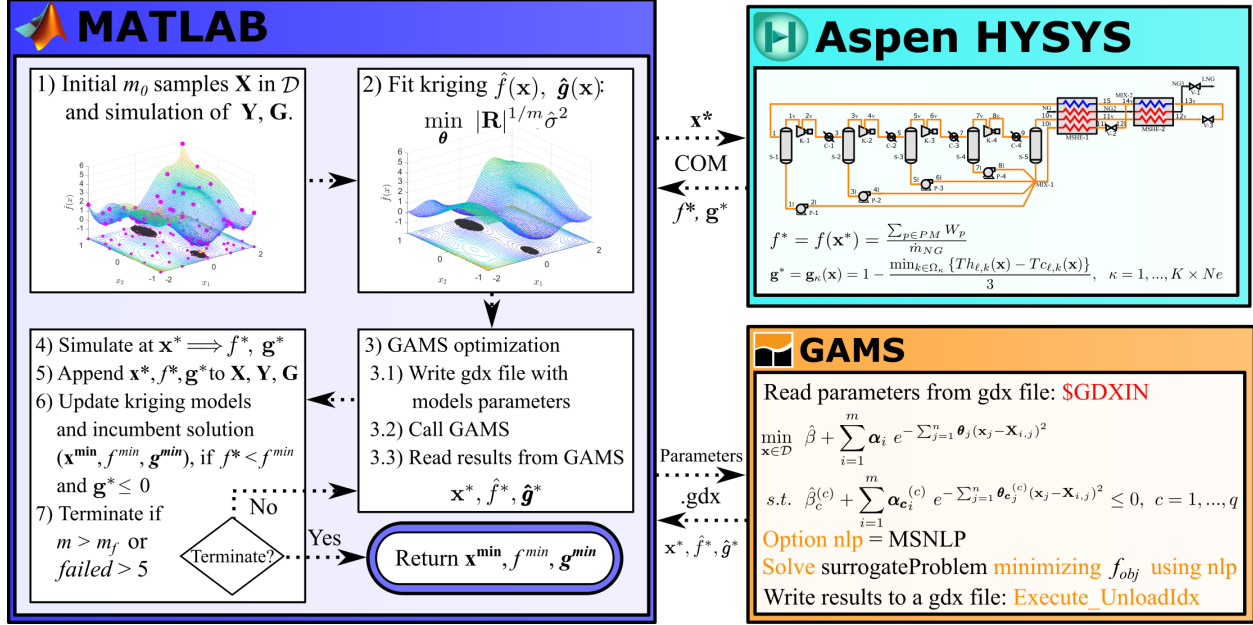


Figure 2: Algorithmic building blocks of present kriging-based optimization framework.

363 variables and methods. In other words, the simulation objects like streams, operations, and solver become
 364 exposed to the programming environment so that each \mathbf{x}^* generated in the MATLAB is sent to the simula-
 365 tion by setting their values in the respective objects features (mass flow rate, temperature, pressure). Then,
 366 after converging the simulation, the objects features that contain the values to calculate the objective and
 367 constraints functions are accessed in the programming environment to compute f^* and \mathbf{g}^* .

368 Then, the first step of this approach is to make an initial sample in \mathcal{D} to adjust the surrogate models.
 369 For that, Latin Hypercube algorithm is used to maximize the minimum distance between points and fill in
 370 m_0 points in the design space. For each sample point in \mathbf{X} , the rigorous simulation is performed to calculate
 371 \mathbf{Y} and \mathbf{G} . Also, the simulation evaluations counter m receives m_0 , $k \leftarrow 0$.

372 Given the initial data \mathbf{X} , \mathbf{Y} , and \mathbf{G} , the kriging models are adjusted for f and \mathbf{g} as in Eq. (10) to
 373 maximize the likelihood of the model given the data. The maximum likelihood optimization problem in Eq.
 374 (9) is solved with the MATLAB implementation of a interior-point method in the built-in function `fmincon`
 375 to determine the θ and θ_c parameters of the kriging models. The initial guess for the algorithm is $\theta_h = 1$ for
 376 $h = 1, \dots, n$. Notice that these parameters are not readjusted, but in between iterations the kriging models
 377 are updated with the same θ to the current \mathbf{X} , \mathbf{Y} , and \mathbf{G} , unless log-likelihood function $\psi(\theta)$ becomes at
 378 least 10 times greater than the value obtained in the adjusting parameter optimization problem in Eq. (9).
 379 In other words, if the model with current parameters is not likely to have generated the available data, a
 380 new parameter adjustment will be performed.

381 Given the kriging models jointly with the maximum likelihood θ parameters, the surrogate optimization
 382 problem as in Eq. (11) is solved in GAMS, where the algebraic kriging models are implemented explicitly.

383 To do that, the programming environment has to communicate with the algebraic modeling language system
 384 to send the model parameters that change every iteration ($\hat{\beta}$, $\hat{\beta}_c$, α , α_c , \mathbf{X} , and possibly θ and θ_c). This
 385 communication is performed via GDX (GAMS Data eXchange) files that provide an interface to read and
 386 write values of GAMS symbols such as sets, parameters, variables, and equations. Then, the GAMS program,
 387 **which** has the surrogate optimization problem implemented, is run from MATLAB to solve the NLP problem
 388 and to write the solution results (\mathbf{x}^* , \hat{f}^* , $\hat{\mathbf{g}}^*$) also in GDX files that are read in MATLAB. Any global solver
 389 that deals with nonconvex NLP problems can be used for this optimization problem. However, there is no
 390 point to spent too much resource and time on global NLP solvers with provable global optimality, such as
 391 Baron [49], because the solution of the surrogate optimization problem in Eq. (11) is an approximation
 392 of the true black-box constrained optimization problem in Eq. (1). Therefore, the multi-start NLP solver
 393 MSNLP from Ugray et al. [50] with CONOPT [51] solver for local search is selected, and the reasoning
 394 behind this choice is that it is fast to converge to (at least) a good local minimizer. The starting points in
 395 the multi-start approach are generated using a normal probability distribution from an initial coarse search
 396 to define a promising region within which random starting points are concentrated.

397 After solving the surrogate optimization problem, the rigorous simulation is performed at the solution
 398 returned to the programming environment from GAMS \mathbf{x}^* to calculate f^* and \mathbf{g}^* , and the simulation
 399 evaluations counter m is iterated. Then, the current values of \mathbf{x}^* , f^* , and \mathbf{g}^* are appended to the data \mathbf{X} ,
 400 \mathbf{Y} , and \mathbf{G} , and the incumbent solution (\mathbf{x}^{min} , f^{min} , \mathbf{g}^{min}) is updated if the solution is improved ($f^* < f^{min}$
 401 and $\mathbf{g}^* \leq 0$). From the extended data, the kriging models parameters $\hat{\beta}$, $\hat{\beta}_c$, α , and α_c are updated and
 402 the algorithm iterates until the maximum number of sampled points m_f **is achieved** or if the surrogate
 403 optimization fails ($f^* > f^{min}$ even for infeasible $\mathbf{g}^* > 0$) five times to provide a promising candidate to solve
 404 the true black-box optimization problem.

405 5. Results

406 In this section, the results from the kriging-based optimization framework proposed in Section 4 applied
407 to the optimal design of single-mixed refrigerant natural gas liquefaction processes with 1, 2, and 3 expansion
408 stages are reported. The considered parameters of the optimization approach are initial sample size $m_0 =$
409 $10n$, which is a classical number for the kriging surrogate model [9], maximum number of samples (function
410 evaluation budget) $m_f = 20n$, number of decision variables $n = 7 + Ne - 1$, number of sections **into which**
411 each multi-stream heat exchanger is divided $K = 10$. The box-constrained design space \mathcal{D} is given by the
412 lower and upper bounds on the decision variables at Table 2, and the computer program to compute f and
413 \mathbf{g} is the natural gas liquefaction processes simulations in Aspen HYSYS. **The computer used to run this**
414 **framework has a Intel Core i7-9750H processor with 16 GB of RAM.**

415 Table 3 presents the best results of decision variables, and objective function from **five** optimization runs
416 for each of the **three** scenarios that accounts for the only randomness present in the proposed framework,
417 which is the initial m_0 samples of \mathbf{X} . The best net work consumption found for these processes are 0.2571,
418 0.2262, and 0.2193 kW per kilogram of natural gas being liquefied per hour, respectively for scenarios (i), (ii),
419 and (iii). It represents a specific net work consumption of 925.5, 814.2, and 789.3 kJ per kilogram of natural
420 gas. These quantitative results show the effectiveness of the optimization framework to find energy-effective
421 alternatives to the single-mixed refrigerant natural gas liquefaction process.

422 From the optimization results in Table 3, it is possible to conclude that the single-mixed refrigerant
423 natural gas liquefaction process benefits from more expansion stages from the energy consumption point of
424 view. Not only the net work consumption decreased with the number of expansion stages, but also the total
425 expected size of the multi-stream heat exchangers (UA) decreased from 657.7 to 550.0 and 543.0 kJ/(°C h)
426 and their total heat duty from 2912 to 2545 and 2406 kJ/h. In other words, the inclusion of more expansion
427 stages in the designed liquefaction processes diminished the work consumption, therefore the electricity
428 and compressors size, and diminished the multi-stream heat exchangers with respect to total heat transfer
429 and expected area. These results are both factors of cost-effective as well as energy-efficient process. The
430 main reason behind this improvement is the improved thermodynamic efficiency of the process with more
431 expansion stages. Table 4 presents the results of entropy generation in each operating unit. The reader is
432 invited to see Santos et al. [45] or Smith et al. [52] for more details on the calculation of entropy generation
433 in this analysis.

434 In fact, the total entropy generation is significantly smaller with more expansion stages, from 0.5634 to
435 0.4377 W/°C for scenario (i) and (iii). The most relevant thermodynamic efficiency gain takes place in the
436 compressors, coolers, multi-stream heat exchangers, and mixers. Therefore, the additional expansion stages
437 with phase separation enable formation of intermediary mixed-refrigerant with different composition in each
438 multi-stream heat exchanger and guarantee a better match between composite curves, as presented in Figure
439 3, more efficient inter-cooled compression system, and smoother mixing processes. The phase separation in

Table 3: Optimization results for single-mixed refrigerant natural gas liquefaction with 1, 2, and 3 stages of expansion

Decision variables	Scenario (i)	Scenario (ii)	Scenario (iii)
m_N [kg·h ⁻¹]	0.1429	0.1582	4.633E-2
m_{C1} [kg·h ⁻¹]	0.4167	0.4426	0.4512
m_{C2} [kg·h ⁻¹]	0.8586	0.9533	1.004
m_{C3} [kg·h ⁻¹]	0.8173	1.198	0.8333
m_{iC5} [kg·h ⁻¹]	1.805	1.735	1.609
P_{suc} [kPa]	350.3	282.8	302.2
P_{dis} [kPa]	2944	2660	3654
T_{exp1} [°C]	-	-24.31	-30.08
T_{exp2} [°C]	-	-	-120.2
Optimization results			
Net work consumption $\left[\frac{\text{kJ}}{\text{kg NG}}\right]$	925.5	814.2	789.3
MSHE-1 minimum temperature approach [°C]	3.000	3.003	3.010
MSHE-2 minimum temperature approach [°C]	-	3.003	3.008
MSHE-3 minimum temperature approach [°C]	-	-	3.010
MSHE-1 expected area (UA) $\left[\frac{\text{kJ}}{^\circ\text{C}\cdot\text{h}}\right]$	657.7	223.2	286.1
MSHE-2 expected area (UA) $\left[\frac{\text{kJ}}{^\circ\text{C}\cdot\text{h}}\right]$	-	326.8	231.8
MSHE-3 expected area (UA) $\left[\frac{\text{kJ}}{^\circ\text{C}\cdot\text{h}}\right]$	-	-	25.07
MSHE-1 heat duty [kJ/h]	2912	1315	1271
MSHE-2 heat duty [kJ/h]	-	1230	1007
MSHE-3 heat duty [kJ/h]	-	-	127.7

440 between compression stages appeared only in the last two stages in accordance with previous works [45]. It
441 is because the multi-component refrigerant is too light to condense at lower pressure levels, even though the
442 optimal values of decision variables in Table 3 show preference to heavier compositions of mixed-refrigerant.
443 In scenario (i), 9.34 % of the mass flow rate is compressed in pump P-3 and 27.82 % in P-4. In scenario (ii),
444 11.51 % of the mass flow rate is compressed in P-3 and 21.08 % in the P-4. In scenario (iii), 20.56 % of the
445 mixed-refrigerant mass flow rate is compressed in P-3 and 18.19 % in the P-4. These results are conclusive
446 to show the importance of phase separation in the energy saving in the compressors K-3 and K-4 as 32.59
447 up to 38.75 % of the mixed refrigerant flow rate is removed from compressors system.

448 *Optimization comparison.* Now, in order to evaluate the performance of the proposed optimization method-
449 ology applied to the optimal design of SMR natural gas liquefaction process, its results are compared to
450 the ones from the well-established global optimization meta-heuristics of Particle Swarm Optimization and

Table 4: Entropy generation analysis

Op. Name	Scenario (i)		Scenario (ii)		Scenario (iii)	
	Sgen [W/°C]	%	Sgen [W/°C]	%	Sgen [W/°C]	%
K-1	5.21E-02	9.25	4.66E-02	10.13	4.60E-02	10.51
K-2	5.09E-02	9.03	4.53E-02	9.84	4.44E-02	10.14
K-3	4.58E-02	8.13	4.04E-02	8.78	3.71E-02	8.48
K-4	3.51E-02	6.23	3.27E-02	7.11	2.98E-02	6.81
C-1	2.15E-02	3.82	1.69E-02	3.67	1.88E-02	4.30
C-2	3.03E-02	5.38	2.81E-02	6.11	3.63E-02	8.29
C-3	5.02E-02	8.91	3.89E-02	8.45	3.54E-02	8.09
C-4	3.49E-02	6.19	2.99E-02	6.50	2.93E-02	6.69
MSHE-1	1.06E-01	18.87	4.10E-02	8.91	2.93E-02	6.69
MSHE-2	-	-	6.14E-02	13.34	3.52E-02	8.04
MSHE-3	-	-	-	-	1.14E-02	2.60
V-1	3.84E-02	6.82	3.84E-02	8.35	3.89E-02	8.89
V-2	4.43E-02	7.86	1.04E-02	2.26	1.47E-02	3.36
V-3	-	-	2.53E-02	5.50	1.61E-02	3.68
V-4	-	-	-	-	6.10E-03	1.39
S-1	-	-	-	-	-	-
S-2	-	-	-	-	-	-
S-3	0.00E+00	0.00	0.00E+00	0.00	0.00E+00	0.00
S-4	0.00E+00	0.00	0.00E+00	0.00	0.00E+00	0.00
S-5	0.00E+00	0.00	0.00E+00	0.00	0.00E+00	0.00
S-6	-	-	-	-	0.00E+00	0.00
P-1	-	-	-	-	-	-
P-2	-	-	-	-	-	-
P-3	4.70E-04	0.08	5.25E-04	0.11	1.20E-03	0.27
P-4	9.72E-04	0.17	6.36E-04	0.14	7.31E-04	0.17
MIX-1	3.50E-03	0.62	3.20E-03	0.70	4.80E-03	1.10
MIX-2	4.87E-02	8.64	4.81E-04	0.10	6.80E-04	0.16
MIX-3	-	-	-	-	1.50E-03	0.34
TOTAL	0.5634	100.0	0.4601	100.0	0.4377	100.0

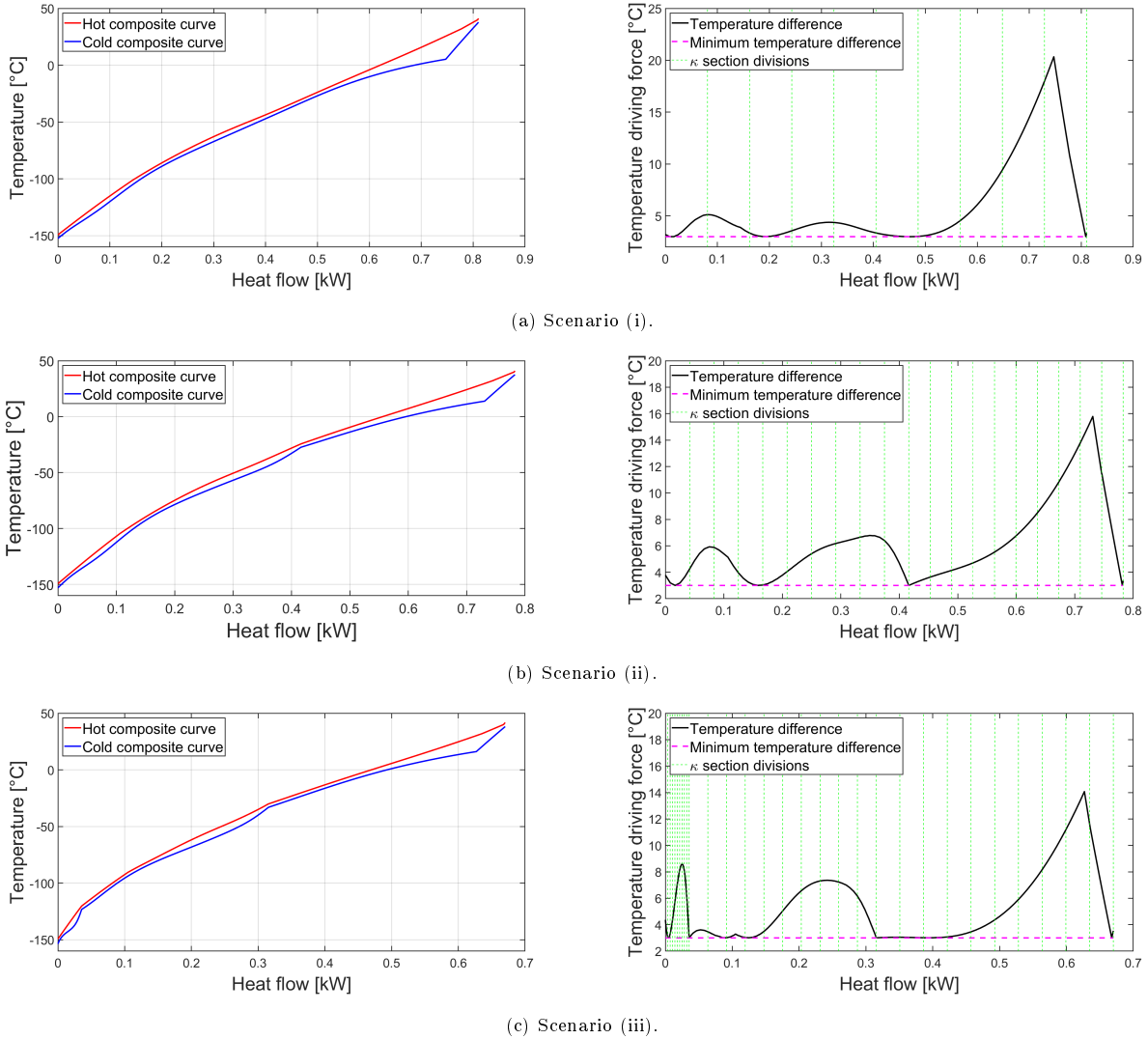


Figure 3: Temperature profiles in the multi-stream heat exchangers

451 Genetic algorithm with the same budget of simulation evaluations, as presented in Table 5. The parameters
 452 were set as default of the MATLAB implementation of these algorithms and with n number of particles,
 453 or individuals, and 20 iterations. To deal with the constraints of the optimization problem in Eq. (13) a
 454 simple barrier penalization is applied proportional to the constraint violation multiplied by a penalization
 455 parameter equal to 1000, as in [45], to guarantee feasible solutions. Knowing that these methods depend on
 456 randomness, each algorithm was applied 5 times for each simulation.

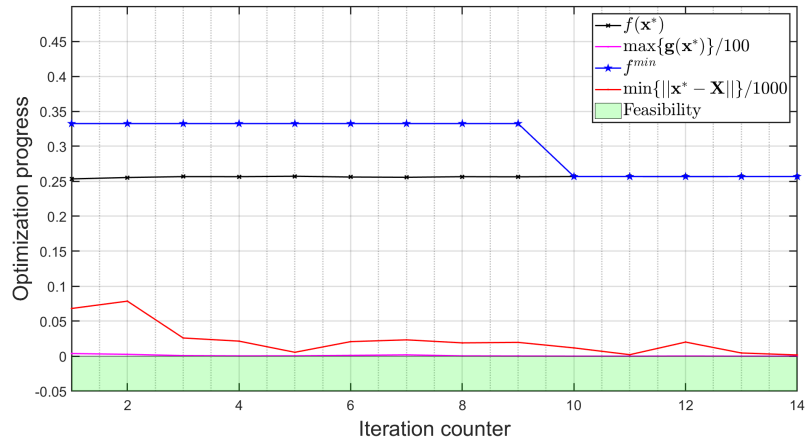
457 From the results in Table 5 it is possible to infer that the present methodology is more efficient (lower
 458 best result of objective function) and more consistent (lower mean value and standard deviation of objective
 459 function) for all three scenarios of the single-mixed refrigerant natural gas liquefaction process design. The
 460 energy savings of the results from the present optimization method in comparison with the ones from Particle

Table 5: Comparison between present optimization framework with PSO and GA

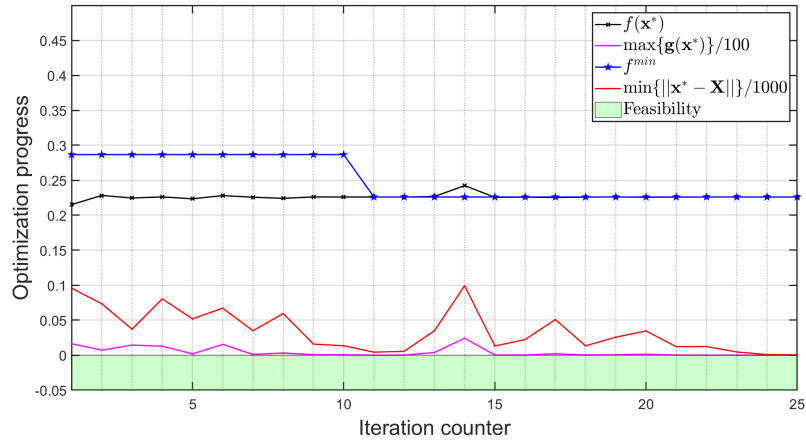
Obj. function		1-stage-expansion SMR			2-stage-expansion SMR			3-stage-expansion SMR		
		Present	PSO	GA	Present	PSO	GA	Present	PSO	GA
Opt. Run	Run 1	0.2571	0.2920	0.2954	0.2262	0.2998	0.3102	0.2198	0.3219	0.3403
	Run 2	0.2572	0.3192	0.3926	0.2262	0.3018	0.2954	0.2200	0.3166	0.3361
	Run 3	0.2571	0.3312	0.3449	0.2262	0.2836	0.2737	0.2203	0.2984	0.3760
	Run 4	0.2571	0.3339	0.4166	0.2272	0.2903	0.4157	0.2197	0.2927	0.3665
	Run 5	0.2571	0.3167	0.3300	0.2262	0.2907	0.3080	0.2193	0.2761	0.3443
Results analysis										
	Best result	0.2571	0.2920	0.2954	0.2262	0.2836	0.2737	0.2193	0.2761	0.3361
	Mean result	0.2571	0.3186	0.3559	0.2264	0.2932	0.3206	0.2198	0.3011	0.3526
	Standard deviation	5.49E-05	1.49E-02	4.36E-02	3.89E-04	6.68E-03	4.93E-02	3.46E-04	1.66E-02	1.57E-02
	Savings (%)	-	12.02	13.03	-	20.29	17.39	-	20.48	34.69
	Execution time (min)	4.22	3.35	4.296	6.25	5.90	5.99	14.05	9.42	9.626

461 Swarm Optimization and Genetic Algorithm are significant, from 12.02 to 34.69 %.

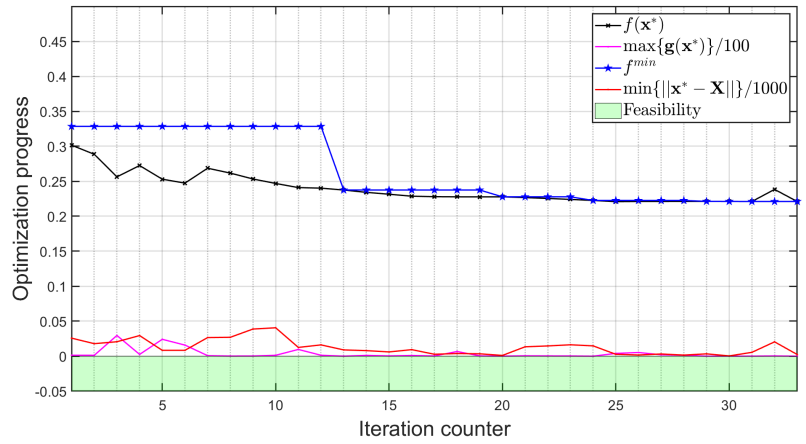
462 Even though the present methodology involves additional steps other than function evaluation and de-
463 termination of next iteration steps, like kriging model fitting and surrogate problem optimization, the mean
464 execution times are competitive with Particle Swarm Optimization and Genetic Algorithm. The first reason
465 for that is due to the computation effort to predict value of f and \mathbf{g} in the kriging surrogate model being
466 way smaller than the simulation. For instance, the mean elapsed time of computing f and \mathbf{g} at the $10n$
467 initial points goes from 1.4 to 3.1 seconds, depending on the simulation, whereas for \hat{f} and $\hat{\mathbf{g}}$ it is in the
468 order of magnitude of 10^{-4} seconds. This allows fast solution time of the surrogate problem in GAMS
469 using multi-start gradient-based local search. The other reason is the convergence of the present approach,
470 illustrated in Figure 4. This convergence is indicated by the objective function value at iterates $f(\mathbf{x}^*)$ (black
471 curve) converging to the incumbent solution f^{min} (blue curve), and the minimum distance of the iterate
472 \mathbf{x}^* to the previous data \mathbf{X} (red line) converging to zero. The optimization progress of the present method
473 is fast because the kriging models capture the behavior of the black-box functions, specially in promising
474 regions (feasible and low values of f). This happens as the sampling comes from the surrogate optimization
475 solution, and is concentrates in these promising regions. One can think of this as an active learning process,
476 where the surrogate models not only learn the black-box functions behavior but also choose where to learn
477 more.



(a) Scenario (i).



(b) Scenario (ii).



(c) Scenario (iii).

Figure 4: Optimization progress of the proposed method for each considered simulation-optimization problem.

478 6. Conclusions

479 This paper presented an optimization framework to solve the constrained black-box simulation optimiza-
480 tion problem that arises from the optimal energy-efficient design of the single-mixed refrigerant natural gas
481 liquefaction process with 1, 2, and 3 expansion stages, using reliable process simulator. In this approach, the
482 kriging model is adjusted to data generated from the process-simulator-dependent, black-box functions of the
483 simulation optimization problem to introduce simple, computationally inexpensive, and effective algebraic
484 formulations to the black-box objective and constraint functions. The constrained surrogate optimization
485 problem is solved in GAMS using state-of-the-art efficient gradient-based multi-start local optimization with
486 CONOPT local solver to determine a candidate of decision variables for which the true functions are calcu-
487 lated in the rigorous simulation. The surrogate problem optimization guides the sampling towards learning
488 the rigorous functions near promising regions for solving the original simulation optimization problem.

489 This optimization framework was applied to the natural gas liquefaction design using the process sim-
490 ulator Aspen HYSYS for rigorous simulations, MATLAB for the main program that handles with linking,
491 data storage, and model fitting, and GAMS for implementing and solving the NLP surrogate optimization
492 problems. The best net work consumption found for these processes are 0.2571, 0.2262, and 0.2193 kW per
493 kilogram of natural gas being liquefied per hour, respectively for scenarios (i), (ii), and (iii), and the total
494 expected size of the multi-stream heat exchangers (UA) decreased from 657.7 to 550.0 and 543.0 kJ/(°C h)
495 and their total heat duty from 2912 to 2545 and 2406 kJ/h. In other words, the inclusion of more expansion
496 stages made the designed liquefaction processes more cost-effective as well as energy-efficient, mainly because
497 of the thermodynamic efficiency of the process.

498 From comparing the present approach to global optimization meta-heuristics of Particle Swarm Optimiza-
499 tion and Genetic Algorithm, it is evident that, for the same budget of simulation evaluations, the present
500 approach is more efficient and more consistent with significant numerical improvement of 12.02 to 34.69 %
501 of energy savings. The main reasons for the better efficiency is the low computation effort to predict the
502 functions f and \mathbf{g} using the kriging surrogate model (from 1.4 to 3.1 seconds in the simulation to the order
503 of magnitude of 10^{-4} seconds for \hat{f} and $\hat{\mathbf{g}}$) that allows fast execution time of the surrogate optimization
504 problem in GAMS. The other reason is the convergence of the present approach, which is relatively fast
505 because the kriging models capture the behavior of the black-box functions, specially in promising regions,
506 and uses it efficiently for optimization.

507 Although it was tested only for single-mixed refrigerant natural gas liquefaction process design, the
508 proposed optimization approach is suitable for any constrained black-box simulation optimization problem,
509 once it provides computationally cheap-to-evaluate surrogate models (kriging) of the objective and constraints
510 functions with simple symbolic formulation that can be embedded to tradition NLP problems.

511 Acknowledgments

512 The authors acknowledge the National Council for Scientific and Technological Development–CNPq
513 (Brazil), processes 148184/2019-7, 440047/2019-6, 311807/2018-6, 428650/2018-0, and Coordination for the
514 Improvement of Higher Education Personnel–CAPES (Brazil) for the financial support.

515 References

- 516 [1] T. W. Simpson, J. D. Peplinski, P. N. Koch, J. K. Allen, Metamodels for computer-based engineering
517 design: Survey and recommendations, *Engineering with Computers* 17 (2) (2001) 129–150. doi:10.
518 1007/PL00007198.
- 519 [2] J. A. Caballero, I. E. Grossmann, An algorithm for the use of surrogate models in modular flowsheet
520 optimization, *AIChE Journal* 54 (10) (2008) 2633–2650. doi:10.1002/aic.11579.
- 521 [3] S. Amaran, N. V. Sahinidis, B. Sharda, S. J. Bury, Simulation optimization: a review of algorithms
522 and applications, *Annals of Operations Research* 240 (1) (2016) 351–380. arXiv:1706.08591, doi:
523 10.1007/s10479-015-2019-x.
- 524 [4] F. Boukouvala, C. A. Floudas, ARGONAUT: Algorithms for Global Optimization of coNstrAined
525 grey-box compUTational problems, *Optimization Letters* 11 (5) (2017) 895–913. doi:10.1007/
526 s11590-016-1028-2.
- 527 [5] A. Bhosekar, M. Ierapetritou, Advances in surrogate based modeling, feasibility analysis, and optimiza-
528 tion: A review, *Computers & Chemical Engineering* 108 (2018) 250–267.
- 529 [6] D. R. Jones, A Taxonomy of Global Optimization Methods Based on Response Surfaces, *Journal of*
530 *Global Optimization* 21 (4) (2001) 345–383. doi:10.1023/A:1012771025575.
- 531 [7] H. J. Kushner, A New Method of Locating the Maximum Point of an Arbitrary Multipeak Curve in the
532 Presence of Noise, *Journal of Basic Engineering* 86 (1) (1964) 97–106. doi:10.1115/1.3653121.
- 533 [8] J. Sacks, W. J. Welch, T. J. Mitchell, H. P. Wynn, Design and Analysis of Computer Experiments,
534 *Statistical Science* 4 (4) (1989) 409–423. doi:10.1214/ss/1177012413.
- 535 [9] D. R. Jones, M. Schonlau, W. J. Welch, Efficient Global Optimization of Expensive Black-Box Functions,
536 *Journal of Global Optimization* 13 (1998) 455–492. doi:10.1023/A:1008306431147.
- 537 [10] M. Schonlau, W. Welch, D. Jones, Global versus local search in constrained optimization of computer
538 models, *Lect Notes Monogr Ser* 34 (1998) 11–25. doi:10.1214/lnms/1215456182.

- 539 [11] D. G. Krige, A Statistical Approach to Some Basic Mine Valuation Problems on the Witwatersrand,
540 Journal of the Chemical, Metallurgical and Mining Society of South Africa (1952) 201–215 [doi:10.
541 2307/3006914](https://doi.org/10.2307/3006914).
- 542 [12] E. Davis, M. Ierapetritou, A kriging method for the solution of nonlinear programs with black-box
543 functions, *AIChE Journal* 53 (8) (2007) 2001–2012. [arXiv:0201037v1](https://arxiv.org/abs/0201037v1), [doi:10.1002/aic.11228](https://doi.org/10.1002/aic.11228).
- 544 [13] A. Cozad, N. V. Sahinidis, D. C. Miller, Learning surrogate models for simulation-based optimization,
545 *AIChE Journal* 60 (6) (2014) 2211–2227. [doi:10.1002/aic.14418](https://doi.org/10.1002/aic.14418).
- 546 [14] Z. Wang, M. Ierapetritou, Constrained optimization of black-box stochastic systems using a novel
547 feasibility enhanced Kriging-based method, *Computers & Chemical Engineering* 118 (2018) 210–223.
548 [doi:10.1016/j.compchemeng.2018.07.016](https://doi.org/10.1016/j.compchemeng.2018.07.016).
- 549 [15] N. Quirante, J. Javaloyes-Antón, J. A. Caballero, Hybrid simulation-equation based synthesis of chemical
550 processes, *Chemical Engineering Research and Design* 132 (2018) 766–784. [doi:10.1016/j.cherd.
551 2018.02.032](https://doi.org/10.1016/j.cherd.2018.02.032).
- 552 [16] A. M. Schweidtmann, A. Mitsos, Deterministic Global Optimization with Artificial Neural Networks
553 Embedded, *Journal of Optimization Theory and Applications* 180 (3) (2019) 925–948. [doi:10.1007/
554 s10957-018-1396-0](https://doi.org/10.1007/s10957-018-1396-0).
- 555 [17] A. Thebelt, J. Kronqvist, M. Mistry, R. M. Lee, N. Sudermann-Merx, R. Misener, ENTMOOT: A
556 Framework for Optimization over Ensemble Tree Models, *arXiv* (mar 2020). [arXiv:2003.04774](https://arxiv.org/abs/2003.04774).
- 557 [18] S. H. Kim, F. Boukouvala, Surrogate-based optimization for mixed-integer nonlinear problems, *Com-
558 puters & Chemical Engineering* 140 (2020) 106847. [doi:10.1016/j.compchemeng.2020.106847](https://doi.org/10.1016/j.compchemeng.2020.106847).
- 559 [19] M. S. Khan, I. Karimi, D. A. Wood, Retrospective and future perspective of natural gas liquefaction
560 and optimization technologies contributing to efficient LNG supply: A review, *Journal of Natural Gas
561 Science and Engineering* 45 (2017) 165–188. [doi:10.1016/j.jngse.2017.04.035](https://doi.org/10.1016/j.jngse.2017.04.035).
- 562 [20] M. A. Qyyum, K. Qadeer, M. Lee, Comprehensive Review of the Design Optimization of Natural Gas
563 Liquefaction Processes: Current Status and Perspectives, *Industrial & Engineering Chemistry Research*
564 57 (17) (2018) 5819–5844. [doi:10.1021/acs.iecr.7b03630](https://doi.org/10.1021/acs.iecr.7b03630).
- 565 [21] International Energy Agency, *World Energy Outlook 2020*, Tech. rep. (2020).
- 566 [22] B. Austbø, S. W. Løvseth, T. Gundersen, Annotated bibliography—Use of optimization in LNG process
567 design and operation, *Computers & Chemical Engineering* 71 (12) (2014) 391–414. [doi:10.1016/j.
568 compchemeng.2014.09.010](https://doi.org/10.1016/j.compchemeng.2014.09.010).

- 569 [23] G. C. Lee, R. Smith, X. X. Zhu, Optimal synthesis of mixed-refrigerant systems for low-temperature
570 processes, *Industrial and Engineering Chemistry Research* 41 (20) (2002) 5016–5028. doi:10.1021/
571 ie020057p.
- 572 [24] F. D. Nogal, J.-K. Kim, S. Perry, R. Smith, Optimal Design of Mixed Refrigerant Cycles, *Industrial &*
573 *Engineering Chemistry Research* 47 (22) (2008) 8724–8740. doi:10.1021/ie800515u.
- 574 [25] A. Aspelund, T. Gundersen, J. Myklebust, M. P. Nowak, A. Tomasgard, An optimization-simulation
575 model for a simple LNG process, *Computers and Chemical Engineering* 34 (10) (2010) 1606–1617.
576 doi:10.1016/j.compchemeng.2009.10.018.
- 577 [26] P. E. Wahl, S. W. Løvseth, M. J. Mølsvik, Optimization of a simple LNG process using sequen-
578 tial quadratic programming, *Computers and Chemical Engineering* 56 (2013) 27–36. doi:10.1016/
579 j.compchemeng.2013.05.001.
- 580 [27] J.-H. Hwang, N.-K. Ku, M.-I. Roh, K.-Y. Lee, Optimal Design of Liquefaction Cycles of Liquefied Nat-
581 ural Gas Floating, Production, Storage, and Offloading Unit Considering Optimal Synthesis, *Industrial*
582 *& Engineering Chemistry Research* 52 (15) (2013) 5341–5356. doi:10.1021/ie301913b.
- 583 [28] M. S. Khan, M. Lee, Design optimization of single mixed refrigerant natural gas liquefaction process
584 using the particle swarm paradigm with nonlinear constraints, *Energy* 49 (1) (2013) 146–155. doi:
585 10.1016/j.energy.2012.11.028.
- 586 [29] T. He, Y. Ju, Design and optimization of a novel mixed refrigerant cycle integrated with ngl recovery
587 process for small-scale lng plant, *Industrial and Engineering Chemistry Research* 53 (13) (2014) 5545–
588 5553. doi:10.1021/ie4040384.
- 589 [30] M. S. Khan, I.A. Karimi, A. Bahadori, M. Lee, Sequential coordinate random search for optimal oper-
590 ation of LNG (liquefied natural gas) plant, *Energy* 89 (2015) 757–767. doi:10.1016/j.energy.2015.
591 06.021.
- 592 [31] P. Moein, M. Sarmad, H. Ebrahimi, M. Zare, S. Pakseresht, S. Z. Vakili, APCI- LNG single mixed
593 refrigerant process for natural gas liquefaction cycle: Analysis and optimization, *Journal of Natural Gas*
594 *Science and Engineering* 26 (2015) 470–479. doi:10.1016/j.jngse.2015.06.040.
- 595 [32] J. H. Park, M. S. Khan, M. Lee, Modified coordinate descent methodology for solving process design op-
596 timization problems: Application to natural gas plant, *Journal of Natural Gas Science and Engineering*
597 27 (2015) 32–41. doi:10.1016/j.jngse.2014.10.014.
- 598 [33] T. N. Pham, M. S. Khan, L. Q. Minh, Y. A. Husmil, A. Bahadori, S. Lee, M. Lee, Optimization
599 of modified single mixed refrigerant process of natural gas liquefaction using multivariate Coggin’s

- 600 algorithm combined with process knowledge, *Journal of Natural Gas Science and Engineering* 33 (2016)
601 731–741. doi:10.1016/j.jngse.2016.06.006.
- 602 [34] J. Na, Y. Lim, C. Han, A modified DIRECT algorithm for hidden constraints in an LNG process
603 optimization, *Energy* 126 (2017) 488–500. doi:10.1016/j.energy.2017.03.047.
- 604 [35] T. N. Pham, N. V. D. Long, S. Lee, M. Lee, Enhancement of single mixed refrigerant natural gas liq-
605 uefaction process through process knowledge inspired optimization and modification, *Applied Thermal*
606 *Engineering* 110 (2017) 1230–1239. doi:10.1016/j.applthermaleng.2016.09.043.
- 607 [36] M. A. Qyyum, W. Ali, N. V. D. Long, M. S. Khan, M. Lee, Energy efficiency enhancement of a
608 single mixed refrigerant LNG process using a novel hydraulic turbine, *Energy* 144 (2018) 968–976.
609 doi:10.1016/j.energy.2017.12.084.
- 610 [37] M. A. Qyyum, N. V. D. Long, L. Q. Minh, M. Lee, Design optimization of single mixed refrigerant
611 LNG process using a hybrid modified coordinate descent algorithm, *Cryogenics* 89 (2018) 131–140.
612 doi:10.1016/j.cryogenics.2017.12.005.
- 613 [38] W. Ali, M. A. Qyyum, K. Qadeer, M. Lee, Energy optimization for single mixed refrigerant natural gas
614 liquefaction process using the metaheuristic vortex search algorithm, *Applied Thermal Engineering* 129
615 (2018) 782–791. doi:10.1016/j.applthermaleng.2017.10.078.
- 616 [39] W. Ali, M. S. Khan, M. A. Qyyum, M. Lee, Surrogate-assisted modeling and optimization of a natural-
617 gas liquefaction plant, *Computers & Chemical Engineering* 118 (2018) 132–142. doi:10.1016/j.
618 compchemeng.2018.08.003.
- 619 [40] W. Lee, J. An, J. M. Lee, Y. Lim, Design of single mixed refrigerant natural gas liquefaction process
620 considering load variation, *Chemical Engineering Research and Design* 139 (2018) 89–103. doi:10.
621 1016/j.cherd.2018.09.017.
- 622 [41] T. He, Z. Liu, Y. Ju, A. M. Parvez, A comprehensive optimization and comparison of modified single
623 mixed refrigerant and parallel nitrogen expansion liquefaction process for small-scale mobile LNG plant,
624 *Energy* 167 (2019) 1–12. doi:10.1016/j.energy.2018.10.169.
- 625 [42] M. A. Qyyum, T. He, K. Qadeer, N. Mao, S. Lee, M. Lee, Dual-effect single-mixed refrigeration cycle:
626 An innovative alternative process for energy-efficient and cost-effective natural gas liquefaction, *Applied*
627 *Energy* 268 (March) (2020) 115022. doi:10.1016/j.apenergy.2020.115022.
- 628 [43] S. Nikkho, M. Abbasi, J. Zahirifar, M. Saedi, A. Vatani, Energy and exergy investigation of two modified
629 single mixed refrigerant processes for natural gas liquefaction, *Computers & Chemical Engineering* 140
630 (2020) 106854. doi:10.1016/j.compchemeng.2020.106854.

- 631 [44] L. F. Santos, C. B. B. Costa, J. A. Caballero, M. A. S. S. Ravagnani, Design and optimization of energy-
632 efficient single mixed refrigerant lng liquefaction process, Brazilian Journal of Chemical Engineering
633 (May 2021). doi:10.1007/s43153-021-00111-8.
- 634 [45] L. F. Santos, C. B. B. Costa, J. A. Caballero, M. A. Ravagnani, Kriging-assisted constrained optimiza-
635 tion of single-mixed refrigerant natural gas liquefaction process, Chemical Engineering Science (2021)
636 116699doi:https://doi.org/10.1016/j.ces.2021.116699.
- 637 [46] L. F. Santos, C. B. Costa, J. A. Caballero, M. A. Ravagnani, Synthesis and optimization of work and
638 heat exchange networks using an MINLP model with a reduced number of decision variables, Applied
639 Energy 262 (2020) 114441. doi:10.1016/j.apenergy.2019.114441.
- 640 [47] S. N. Lophaven, H. B. Nielsen, J. Søndergaard, et al., DACE: a Matlab kriging toolbox, Vol. 2, Citeseer,
641 2002.
- 642 [48] M. L. Stein, Interpolation of spatial data, Springer Series in Statistics, Springer-Verlag, New York, 1999,
643 some theory for Kriging. doi:10.1007/978-1-4612-1494-6.
- 644 [49] M. Tawarmalani, N. V. Sahinidis, A polyhedral branch-and-cut approach to global optimization, Math-
645 ematical programming 103 (2) (2005) 225–249.
- 646 [50] Z. Ugray, L. Lasdon, J. C. Plummer, M. Bussieck, Dynamic filters and randomized drivers for the
647 multi-start global optimization algorithm msnlp, Optimization Methods and Software 24 (4-5) (2009)
648 635–656. doi:10.1080/10556780902912389.
- 649 [51] A. S. Drud, Conopt—a large-scale grg code, ORSA Journal on computing 6 (2) (1994) 207–216.
- 650 [52] J. Smith, N. Smith, H. Van Ness, M. Abbott, M. Swihart, Introduction to Chemical Engineering Ther-
651 modynamics, McGraw-Hill chemical engineering series, McGraw-Hill Education, 2017.